The Influences of Type 1 El Niño and La Niña Events on Streamflows in the Pacific Southwest of the United States

ERCAN KAHYA AND JOHN A. DRACUP

Civil Engineering Department, University of California, Los Angeles, Los Angeles, California

(Manuscript received 10 August 1992, in final form 2 July 1993)

ABSTRACT

Streamflows in the Pacific Southwest of the United States in relation to the tropical Type 1 El Niño–Southern Oscillation (T1ENSO) and La Niña events are examined using composite and harmonic analyses for each event during a 24-month evolution period. The hydroclimatic signals associated with either extreme phase of the Southern Oscillation (SO) are explored based on data from 50 streamflow stations in California, Arizona, New Mexico, Colorado, and Utah. A significant level for the results is assessed by the use of a hypergeometric distribution. Highly significant, coherent signals are demonstrated to exist for both events, with opposite sign and almost identical timing. Pacific Southwest streamflow responses to the T1ENSO thermal forcing are characterized by a wet December–July season in the subsequent year of the event. Similarly, a dry February–July season is detected as a period at which the La Niña–streamflow relationship is strong and spatially coherent. An index time series is plotted to determine the temporal consistency of the signal. It was found that the respective seasonal signal for each event was confirmed by all episodes. Amplification (suppression) of the regional annual streamflow cycle is noticed during the subsequent year of the typical T1ENSO (La Niña) event.

A lag cross-correlation analysis is conducted between the time series of the seasonal December–July streamflow index and the SO index. The March–May season in the previous year of the seasonal T1ENSO signal was determined to be the logical period in which the SO index can be averaged to obtain the highest correlation and the maximum time lag. A Mann–Whitney U test reveals statistically significant differences in the means of seasonal streamflows associated with T1ENSO and La Niña events. Plausible explanations for the observed teleconnections are presented.

1. Introduction

Despite the confusing terminology regarding the extreme phases of the Southern Oscillation (SO) (Aceituno 1992), the terms El Niño, warm event, and El Niño–Southern Oscillation (ENSO) are used interchangeably in this paper. The amplitudes of different El Niño events vary dramatically, as evident in the time series of the SO index (SOI) and in the sequences of sea surface temperature (SST) anomalies off the coast of South America during warm events (Rasmusson and Carpenter 1982). The occurrence of an El Niño event is quantified in four categories: strong, moderate, weak, and very weak. Episodes within the same category, however, differ noticeably in terms of intensity, timing, and influences (Quinn et al. 1978). The strong 1982–83 ENSO episode led Fu et al. (1986) to describe three types, or profiles, of ENSO patterns based on zonal SST distribution within the equatorial Pacific band of 4°N–4°S, 120°E–80°W during the development stage. Type 1 events, which are the central interest of this study, can be described during the June–August season as (i) much warmer than normal ocean surface water located easterly of the international date line, (ii) close to normal conditions in the western Pacific, and (iii) the warmest water stretching from the eastern Pacific to 150°–160°W longitude. There have been seven Type 1 events documented since 1950 (Schonher and Nicholson 1989). Fu et al. (1986) state that the eastward migration of the warm water pool in the western Pacific and the change of east–west SST gradient for distinct patterns result in different types of atmospheric circulation patterns. As a result, it is also reasonable to expect different patterns of climatic surface parameters that are believed to be teleconnected to the state of the climate over the equatorial Pacific.

A few recent studies exist concerning climatic variables in association with the intensity or type of the tropical ENSO phenomena. A study by Andrade and Sellers (1988) on the influences of the El Niño events on Arizona precipitation revealed episodes having an impact on both seasonal and annual precipitation. Schonher and Nicholson (1989) examined the spatial and temporal modulation of annual California rainfall patterns by the ENSO forcing and evaluated their results in conjunction with the types of warm events.

Corresponding author address: Dr. John A. Dracup, Civil Engineering Department, University of California, Los Angeles, 405 Hilgard Avenue, Los Angeles, CA 90024-1593.

They emphasize that Type 1 episodes invariably produce wet conditions statewide over California.

Kahya and Dracup (1993a, hereafter KD) present analysis results concerning the existence of ENSO–streamflow relationships using data from 1009 streamflow stations throughout the contiguous United States. They identified four core areas that have strong consistent relationships between streamflow and ENSO (warm) events, namely, the Gulf of Mexico (GM), the Northeast (NE), the North Central (NC), and the Pacific Northwest (PNW). A typical seasonal ENSO signal for each region may be expected during the event year as a wet period of December–April for the GM, a dry period of August–February for the NE, a wet period of April–January for the NC, and a dry period of May–October during the subsequent year for the PNW region. The Southwest region described in KD (Fig. 1), which was based on the composite analysis without discriminating the type of an ENSO event, did not qualify as a core area. However, the ENSO–streamflow relationship appeared to be consistent for the Type 1 subset of ENSO events (see Fig. 9 of KD). Furthermore, Kahya and Dracup (1993b) analyzed the linkages between California streamflows and three types of ENSO events and indicate coherent modulation of streamflow anomalies by Type 1 ENSO (T1ENSO) forcing statewide. They found regionally specific responses over California and an excellent association between streamflow and T1ENSO events in the southern part of the state, which represents the western half of the Southwest region in KD.

The modulation of hydroclimatology and enhanced precipitation variability in the southwestern United States, especially Arizona, are attributed to tropical ENSO forcing (Webb and Betancourt 1990; Cayan and Webb 1992). The impact of moderate or strong warm events on the precipitation field in Arizona and western New Mexico is more pronounced for the normally dry spring and fall seasons because of unusual SST anomalies extending to the west coasts of California and Mexico (Andrade and Sellers 1988). The biennial tendency and the opposite SO-related response during a warm phase to that during a cold phase have been indicated by Kiladis and Diaz (1989) for the Southwestern precipitation.

Because the southwestern United States appears to have a more reliable relationship to T1ENSO than the other ENSO types, we were interested in only T1ENSO episodes and their influence on streamflow anomalies. Since a streamflow–SOI correlation pattern suggests a larger areal influence (Cayan and Peterson 1989), we analyzed a larger geographical area than the Southwest region that was identified by KD to designate the southwestern United States. We also included a diagnosis of streamflow anomaly fluctuations during cold (La Niña) events with a lifetime period of 24 months within the same region.

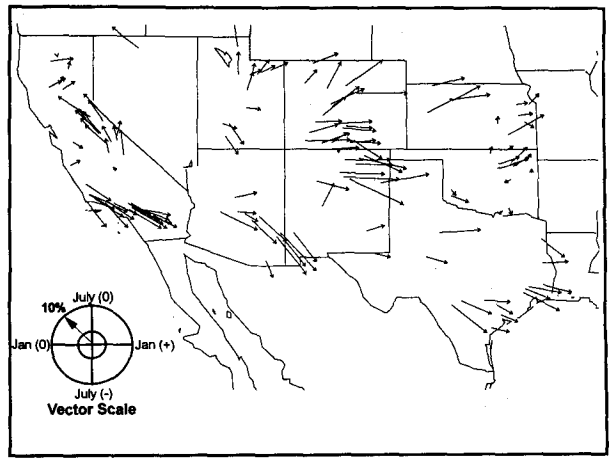

FIG. 1. First harmonic vectors extracted from a 24-month ENSO streamflow composite based on nine events without discriminating the type of event in the southwest United States. Scale for the direction of arrows: south refers to July (−), west refers to January (0), north refers to July (0), and east refers to January (+). Adopted from Kahya and Dracup (1993).

2. Dataset and methodology

Monthly unimpaired streamflow amounts used in this study are extracted from a dataset that was compiled by Wallis et al. (1991). The dataset contains 133 high quality streamflow records in California, Arizona, New Mexico, Texas, Oklahoma, Kansas, Colorado, Utah, and Nevada. Each record contains 41 years of observation, from October 1948 to September 1988. According to Table 4 of Schonher and Nicholson (1989), this period contains a total of seven T1ENSO episodes: 1951, 1957, 1965, 1968, 1972, 1977, and 1982. Two episodes, 1968 and 1977, were not included in KD. Eight La Niña events occurred during the study period: 1950, 1955, 1956, 1964, 1970, 1971, 1973, and 1975. Ropelewski and Halpert (1989) identified these years as La Niña events; the years are in good agreement with the high/dry years of van Loon and Madden (1981). In this study, La Niñas are defined as events occurring when the SOI (Tahiti–Darwin) remains in the upper 25% of the distribution for five months or longer (Ropelewski and Jones 1987). It should be noted that the terms SO, El Niño, and La Niña are general and qualitative (Philander 1990), and the definition of these terms vary widely.

A technique similar to that used by KD is adapted. The analysis starts with a transformation of original records into percentiles based on a lognormal distribution for each month at each station. Using this transformation, all streamflow records having a different original mean and variance are put on an equal basis. Following the analysis of Ropelewski and Halpert (1986, 1989), a 2-yr period is chosen to represent a lifetime period for the T1ENSO and La Niña events.

Using common conventions, the T1ENSO (La Niña) year is designated by (0), while the year before is (−), and the year after is (+). A 24-month percentile composite based on the seven T1ENSO episodes is then established for each individual station. The first harmonic extracted from such a composite is represented as a harmonic dial and then mapped (Fig. 2) to identify a core region of spatially coherent streamflow responses to the T1ENSO forcing within the Southwest.

The amplitude and phase of a harmonic dial refer to the strength and time of the response, respectively. That is, the amplitude refers to a representative magnitude of seasonal streamflow anomalies assumed to fluctuate in relation to the T1ENSO phenomena. The phase indicates the timing of this fluctuation or the time at which the first harmonic has a maximum departure from the composite mean. The harmonic analysis and the advantages of using a harmonic dial (vector) are discussed in Rayner (1971) and Conrad and Pollak (1950). The maximum or minimum value of the first harmonic is assumed to represent a T1ENSO signal. This assumption can be related to a biennial tendency in the fluctuation of climatic variables that are considered to be affected by the SO (Kiladis and Diaz 1989). The statistical significance of the harmonic amplitude and phase are assigned by the use of Schuster's test for an autocorrelated series and by the vectorial coherence. The vectorial coherence is used to determine regions of coherent harmonic vectors and is defined as the ratio of the vector mean to the scalar mean. The concept of coherence is defined and discussed in KD.

The Pacific Southwest (PSW) area, outlined in Fig. 2, was designated as a core region. This area covers Arizona and California (excluding the area east of Sierra Nevada), eastern New Mexico, a small southwestern portion of Colorado, and southern Utah. This specific boundary identification was based on a comparison of individual T1ENSO composites to those with similar anomaly fluctuations. Because of the similar positioning of vectors in Fig. 2, two more scenarios regarding the geographical extent were analyzed. The first scenario was the inclusion of eastern Colorado into the PSW, and the second was the exclusion of Utah from the PSW. Neither scenario improved the results that were obtained for the area depicted in Fig. 2.

All individual T1ENSO composites within the PSW, each having a 3-yr period, are averaged together to obtain an aggregate composite. This is subjected to the detection of a seasonal T1ENSO signal. The reason for using a 3-yr period is to observe more accurately the duration of the signal and to determine whether it extends beyond June (+). Finally, an index time series (ITS) based on the season previously detected is formed to examine the reliability of the T1ENSO–streamflow relationship. The ITS consists of two averaging processes. First, a spatial average of the monthly percentile values for all stations within the PSW is obtained, and

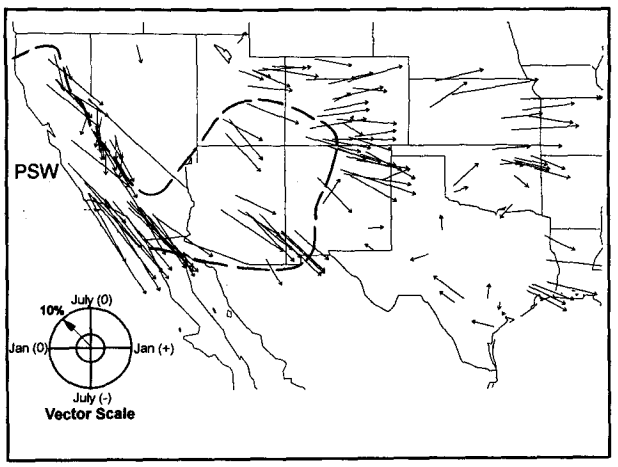

FIG. 2. Same as in Fig. 1 but with composites based on seven T1ENSO events. The PSW region is outlined by the dashed lines. The difference from Fig. 1 with respect to the magnitude and phase coherency of the vectors in the PSW is obvious.

second, a temporal average is obtained for the months in the detected season using the spatially averaged series.

In examining the relationship between streamflow and La Niña events (positive index phase of the SO) in the PSW, the same procedure outlined above is performed using six La Niña years (1950, 1955, 1964, 1970, 1973, and 1975). In cases of two successive La Niña episodes (1955, 1956 and 1970, 1971), only the first year is used for the individual station composite. The second years (1956, 1971) are marked in the ITS, however. Some statistical techniques characterizing features of the SO-related signals are provided, along with their results, in section 4.

3. Results and discussions

The PSW region contains 50 stations over the five aforementioned states. The vectorial coherence computed for all first harmonic dials in the PSW region (Fig. 2) is 0.97, indicating all vectors pointing almost the same direction or having a similar phase. This high percentage of coherence indicates that all stations have similar timing of maximum (or minimum) and are spatially coherent in terms of fluctuations during the evolution of T1ENSO events. Figure 1 depicts a map of harmonic vectors calculated from nine ENSO episodes without distinguishing any type. The large amplitude and phase coherence are the noticeable differences between Fig. 1 and Fig. 2. This reveals a more consistent and reliable relationship between streamflow and T1ENSO events. The significance levels for the amplitudes of harmonics based on Schuster's test are quite impressive. For T1ENSO events, 17 out of 50 harmonic vectors had a significance level lower than

0.01. This means that there is less than a one percent chance of obtaining the first harmonic by random fluctuations. Twenty-two vectors had a value between 0.01 and 0.10, and the remaining 11 vectors had a value less than 0.24. In addition to these strong significance levels, the percentage of the explained variance by the first harmonic was, on the average, 63% (ranging from 39% to 84%) for each individual T1ENSO composite. This is consistent with the assumption of a biennial variation in the streamflow anomalies during the lifetime of a typical episode.

Figure 3a illustrates that negative anomalies during years (−) and (0) are followed by a period of highly wet departures whose onset is concurrent with the mature phase of warm events (Rasmusson and Carpenter 1982). A single season representing a T1ENSO signal is selected as December (0) to July (+) for the PSW region (shown by the dashed lines in Fig. 3a). To determine this season, we reexamined streamflow anomaly sequences of each station within the PSW region during years (0) and (+) and illustrated only the dominant positive departures from the median month by

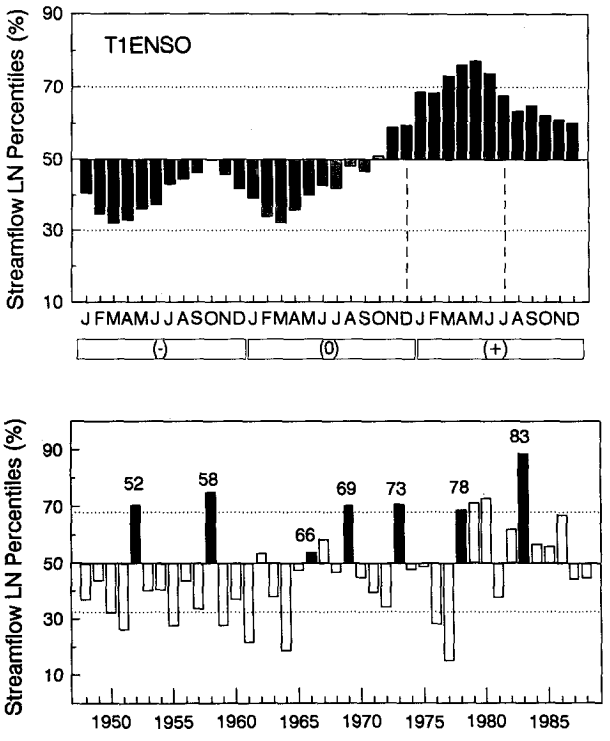

FIG. 3. (a) Aggregate composite based on the percentiles of lognormal distribution for the PSW region. The dashed lines delineate a season of possible T1ENSO-related streamflow response. The months in the box refer to T1ENSO or year (0). (b) Relevant index time series for the wet season from December (0) to July (+) detected in (a). The ordinate values represent the spatial average of streamflow percentiles for all stations within the PSW region. The year in which the seasonal T1ENSO signal occurs is shown by dark bar. Of the seven T1ENSO episodes, all departures from the median are positive.

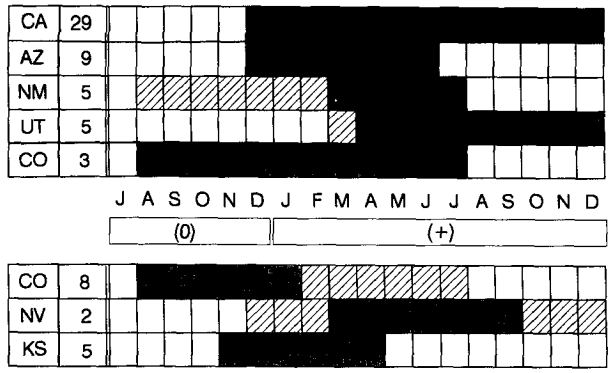

FIG. 4. Months that had wet streamflow anomalies (shown by dots) during July (0) to December (+) observed in the individual station composite for statewide subregions in the PSW. The number in the second column refers to the number of stations in the part of the state covered by the PSW that demonstrated monthly wet anomalies as depicted in the rest of the figure. Months showing dashed lines are most likely wet for the majority of the stations. As an example, for the third line, five stations in New Mexico are covered by the PSW; in these five station T1ENSO composites, apparent wet streamflow anomalies occurred during the March(+)–July(+) season, and in most of five station composites, the August(0)–February(+) season exhibited weak-to-moderate wet anomalies.

month in Fig. 4. The dotted months in the figure exhibited noticeable wet anomalies common to those T1ENSO composites whose quantity is shown in the second column for each state. The hatched months indicate that most of the stations had weak-to-moderate wet anomalies. The top block in Fig. 4 suggests that the December (0)–July (+) season is the logical choice, revealing a common period for all five states. We also included the regions of midwestern Colorado, Nevada, and mideastern Kansas, shown in the lower block of Fig. 4, to give an idea about the typical streamflow fluctuations during years (0) and (+). Texas and Oklahoma were not shown because of the occurrence of inconsistent negative anomalies during year (+). The strong positive anomalies after July (+) in Fig. 3a are attributed to the contribution of streamflows in California and Utah.

To make sure that the December–July season is temporally germane to the hypothesized tropical thermal forcing, the ITS is plotted (Fig. 3b) to see whether a consistent relationship exists between streamflow and T1ENSO phenomena. All the ITS values (seasonal streamflow lognormal percentiles) during year (+)—for example, 1952 for the 1951 episode—demonstrated a positive departure, thus providing 100% confirmation. The empirical probability that the period of December–July in any year is above the median is 0.36. Six of the eight wettest cases, however, were above the 67.7 percentile (a threshold for the highest 20% of the distribution of ITS values) and occurred in conjunction with T1ENSO events. In the 41-yr study period, 1983 is the only year having 12 months above the median.

All of these 12 months had a percentile value equal to or greater than 81. Furthermore, the wettest (88.8 percentile) season in the ITS coincided with the 1982–83 episode, which was the most intense warm event in this century. Using spatially averaged time series of 50 streamflow records, a visual inspection of the months between December and October for the year (+) of T1ENSO episodes revealed that no individual episode dominated the identified signal. This is also implied by the high level of consistency.

Figure 5a illustrates an aggregate La Niña composite for the PSW region. The timing and magnitude of anomaly sequences during the months of years (0) and (+) appear almost similar to those during (−) and (0) in the T1ENSO composite. Again, largest absolute anomaly magnitudes occur during year (+), and an apparent La Niña signal is identified as a dry season of February (+) to July (+). The corresponding ITS in Fig. 5b shows that all eight La Niña occurrences have confirmed this seasonal signal. Three of the eight driest cases, which are below the 31.9 percentile (a threshold for the lowest 20% of the distribution of ITS values), are coincident with the cold events.

Comparing both ITSs (Fig. 3b and Fig. 5b) with respect to magnitude, the T1ENSO signal is stronger than the La Niña signal. This is especially true for the extreme streamflow conditions, which will also be tested statistically in the following section. Minor dissimilarities between Fig. 3b and Fig. 5b are due to the fact that the months included in both signals (Fig. 3a and Fig. 5a) are not exactly the same. Therefore, the seasonal average for each year becomes slightly different for the ITSs. One interesting feature of Fig. 3b is that on an interannual time scale the wet seasons associated with the years subsequent to the 1951, 1957, 1972, and 1977 episodes have an unorthodox appearance. Although our sample size is too small to generalize, in these four cases a T1ENSO event interrupts prevailing dry spells. Similarly, La Niña events characterize and maintain dry conditions in the PSW region, as evident by the February–July season's association with dry spells. Similar situations were noted for precipitation along the coast of northern Peru (Aceituno 1992).

Here our results are compared to those of an analysis of precipitation and temperature by Kiladis and Diaz (1989) for the southwestern United States. One difference is that our composite analysis for the low index phase of the SO is based on only T1ENSO events, and their analysis did not distinguish the type of ENSO events. They defined the signal, which is associated with the extremes of the SO in precipitation or temperature data, as t-value significant at the 0.05 level for the difference in the means of warm and cold event composites of each standard season at a station. Kiladis and Diaz found weak wet anomalies in the fall of year (0) and inconsistent dry anomalies in the fall of year (−)—that is, one year earlier than most parts of the

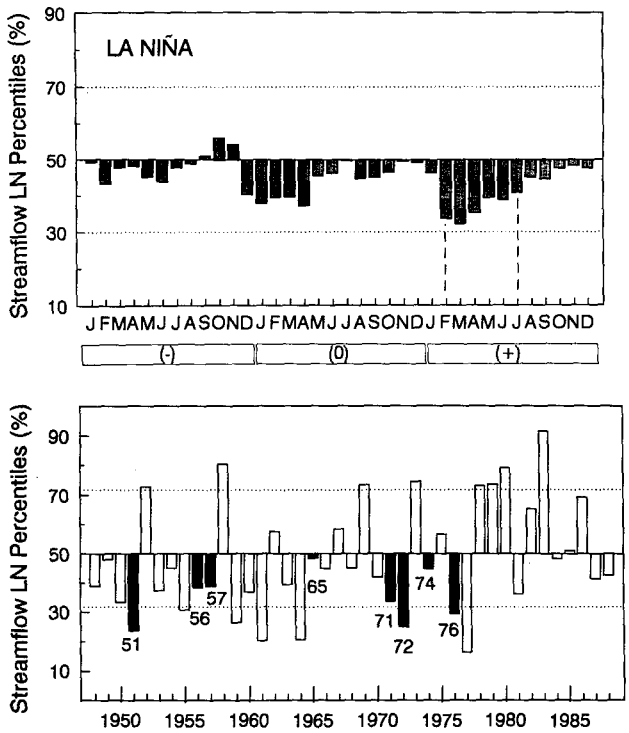

FIG. 5. Same as in Fig. 3 but for La Niña events. A seasonal signal is selected as a dry period of February (+) to July (+). In the corresponding index time series, all eight episodes confirm the signal.

PSW. This was considered to support one of their hypotheses, which is the opposition of the SO-related signals between composite year (−) and year (0) for warm and cold events. Interestingly, the fall seasons of years (−) and (0) in Fig. 3a are observed as a transition period for streamflow anomalies to follow, a remarkable reversal of sign from during the December–July period. A weak unreliable wet signal was noted during summer of year (0). This signal persists into the following fall season with a higher level of significance. The response of streamflow to these weak positive precipitation anomalies in these two consecutive seasons appears as early as November (0) (Fig. 3a). In the eastern border of the PSW region, Kiladis and Diaz found strong wet anomalies in the winter of year (0) that persist into the spring of year (+) covering the eastern half of the PSW. The Southwest winter precipitation maximum occurs in January–February (Cayan and Peterson 1989). Most of the streamflows in the eastern PSW are located in a high elevated basin (Wallis et al. 1991). Taking these factors into account, streamflow responded strongly to the winter and spring positive precipitation anomalies during the previously identified T1ENSO seasonal signal. The opposite of the indications given above characterizes the signal of cold events. These indications concerning years (0) and (+) are consistent with composite streamflow anom-

alies in Fig. 5a. Using the Salt River basin of Arizona as a prototype Cayan and Webb (1992) reason that an increase (decrease) in the frequency and the amount of daily precipitation during early winter of year (+) (November–January) and late winter (+) (February–April) are responsible for the increased (decreased) streamflow in year (+) of El Niño (La Niña).

Furthermore, Kiladis and Diaz did not notice a strong significant temperature signal for the entire PSW in any season within the event evolution period, except for the warm conditions observed during the fall of year (0) and the winter of year (+) in the western PSW. They also point out that there is almost uniform reversal in the sign of precipitation and temperature anomalies between warm and cold events in regions displaying a strong signal. Ropelewski and Halpert (1987, 1989) indicate similar opposition in anomaly sign of the same climatic surface parameters for 15 of 19 core regions over the globe. This reversal is obviously confirmed by the Pacific Southwestern streamflow responses to the corresponding tropical events.

Webb and Betancourt (1990) state that at the time of certain ENSO phenomena, frontal storms in winter become more intense and numerous in the PSW region because of the intensification of the Aleutian low. Significant changes in the variability of tropical cyclone generation during ENSO events, which are possibly affected by the presence of warm SST off the west coast of Mexico and California (Andrade and Sellers 1988), are reflected as more frequent tropical cyclones dissipating over Arizona. Positive correlations between summer Line Island and the Southwestern precipitation observed by Douglas and Englehart (1984) are significant during the months following summertime (e.g., October, November, February, and March), when the dominance of cutoff low pressure systems at the 500-mb level generally increases during ENSO events.

Ely et al. (1992) studied the composite daily 700-mb and monthly sea level geopotential height anomalies in association with floods that occurred in the six subregions of the southwestern United States. The dominant flood-producing circulation pattern in the winter is a low pressure anomaly off the California coast and a high pressure anomaly over the Gulf of Alaska. The daily atmospheric circulation patterns at 700 mb associated with winter floods are often so persistent or strong that they dominate the magnitude of the monthly sea level pressure. Similarly, Ely et al. indicate that a few large flooding episodes contribute to the significant portion of total annual streamflow rivers in the Southwest. At least one flooding event has been observed in all their six subregions, and they happened during the period of wet T1ENSO signal identified by this analysis (see their Table 1). For example, between years 1948 and 1988, the Mojave subregion experienced flood events in three of four cases, and the North Gila revealed three of eight cases.

Andrade and Sellers (1988) conclude that increased precipitation in normally dry spring and fall seasons is caused by the invasion of anomalously warm water off the West Coast during El Niño events. This warm water is the source of necessary energy for the development of strong troughs. In the region of the trade winds and particularly near 20° latitude, air often sinks because of the subtropical high, becomes warmer, and consequently generates the trade wind inversion. The warm water weakens this inversion, allowing more moisture-laden air to enter over the Southwest. Precipitation during winter is less dependent on this warm water, but intense middle-latitude storm systems still produce abundant precipitation. It should be noted that the forcing of the large-scale circulation over the Pacific Ocean by tropical heating is a more significant factor. Taking storage effects into consideration, the reasoning of Andrade and Sellers is consistent with our results in that the wet T1ENSO seasonal signal has been observed from winter to the end of the summer season.

Hales (1974) indicates that a large-scale sea-breeze mechanism is in effect during the summer in the Gulf of California and in the desert Southwest. Since the Gulf of California is a relatively smooth path for northward-moving tropical air masses, topographic influences (such as the Sierra Madre in western Mexico and the Mogollon Rim in southern Arizona) play an important role in determining the distribution of precipitation during the July–August season. For example, these factors cause southeastern Arizona to become wetter than southwestern New Mexico. Since the source of moisture in the Southwest during summer originates in the tropical Pacific, we speculate that negative summer streamflow anomalies in the ENSO year may be due to a decrease in the temperature gradient between ocean and land. The opposite situation (a strong temperature gradient) produces above-the-median streamflow anomalies during summer of the subsequent year of the ENSO events.

The teleconnection may also be related to cloudiness. Angell and Korshover (1987) found a significant increase in Southwest cloudiness, a combined parameter of cloud amount and sunshine duration, between 1950 and 1985. United States cloudiness is 5% above average during strong T1ENSO events, such as the 1972 and 1982 episodes. In contrast, there is a tendency toward below-average U.S. cloudiness at the time of La Niña events. The Southwest is one of two regions in the contiguous United States where a significant cloudiness correlation to the SST variations in the equatorial Pacific has been shown. Additionally, Douglas and Englehart (1981), who found significant correlation between Southwestern winter precipitation and the equatorial fall rainfall index, emphasize the importance

of eastward moving low-latitude troughs and associated tropical cloudiness in the teleconnection.

4. Further analyses

a. Seasonal cycles

Most streamflows in the western United States reveal a strong seasonal variation in monthly means, following precipitation and temperature influences (Cayan and Peterson 1989). A harmonic analysis is an objective technique to determine the annual and semiannual cycles. A good discussion concerning harmonic analysis in evaluating periodicity was presented in Rayner (1971) and Scott and Shulman (1979). Cayan and Peterson (1989) showed the annual streamflow cycle harmonic dials for a larger (but coarser) grid than was used in this study over the western United States, Canada, and Alaska. Briefly, at an individual station, monthly streamflow values are averaged over the 41-yr period to obtain 12 monthly mean values. This resulting series is subjected to harmonic analysis to extract the first and second harmonics. As in section 3, these two sine curves are presented as a vector whose direction and length correspond to the phase and amplitude of the harmonics, respectively (Hsu and Wallace 1976). Then all the harmonics are plotted on a map to establish a spatial outlook of streamflow regimes. A percentage value of standardized variance (SV), computed from (1), is represented by the length of harmonic vector, indicating the magnitude of the seasonal maximum:

$$SV = \frac{C^2}{2s^2}, \qquad (1)$$

where C is the row amplitude of the harmonic under consideration (i.e., first or second harmonic), and s is the unbiased estimate of standard deviation for the 12 monthly mean series. In this convention, SV takes a value between zero and one and corresponds to the explained portion of total variance (s^2) by that particular harmonic. A higher SV value means a better harmonic fit and a strong implied cycle within the entire streamflow records.

Figure 6a (Fig. 6b) shows the distribution of the first (second) harmonics in the southwestern United States. A strong annual cycle dominates streamflow oscillations with an approximate SV value of 0.60, and the time of maximum occurs roughly during March. The semiannual cycles are very weak, but the time of first maximum appears to be in phase with that of the first harmonic. Interestingly, the PSW, except its northern part, is geographically distinguishable in the maps of annual and semiannual cycles (Fig. 6), since the vectors outside of the region point in quite different directions than those within the region.

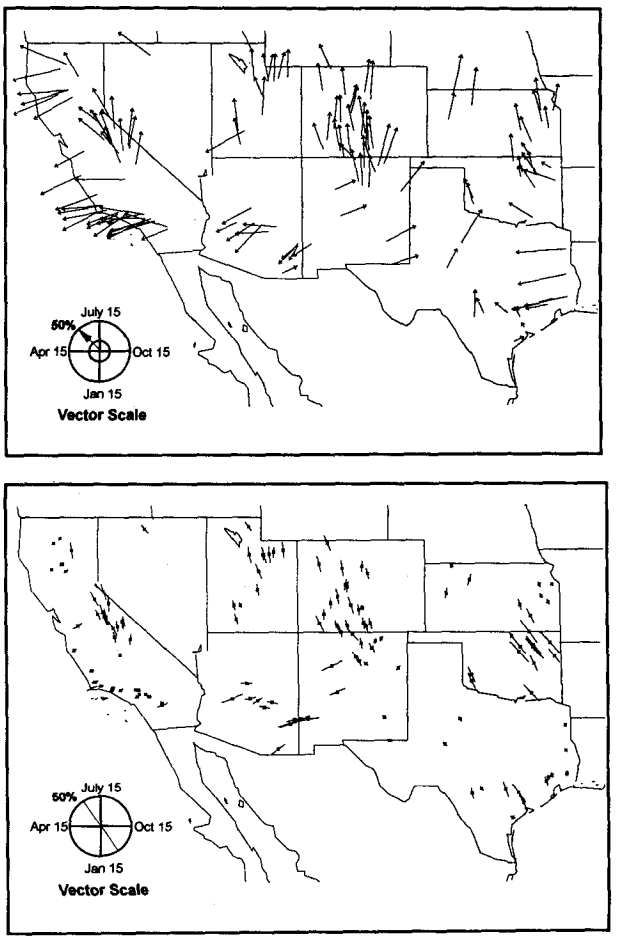

FIG. 6. (a) The annual streamflow cycles in the rivers of the PSW region. Scale for the direction of arrows: south refers to 15 January, west refers to 15 April, north refers to 15 July, and east refers to 15 October. (b) Same as in (a) except for the semiannual cycles.

In this context, a question is raised regarding streamflow fluctuations during the evolution of both SO extreme events in comparison with the annual cycle. It is also important to know whether the SO-related signals occurred during the peak or minimum flow. For this purpose, instead of dealing with each individual station, three regional time series are formed: the annual cycle, the T1ENSO, and La Niña. Both composites have a 36-month period and cover the entire (−), (0), and (+) years. To diminish the effect of dispersed mean and variance values across the PSW region, each monthly value of all 41 years is transformed to a modular coefficient at each station. This is simply a way to express monthly streamflow values in terms of the percent of mean annual streamflow and to preserve the seasonal cycles. Then these modular coefficients are spatially averaged month by month for 50 stations to obtain a regional monthly time series. From this resulting series, T1ENSO and La Niña composites are

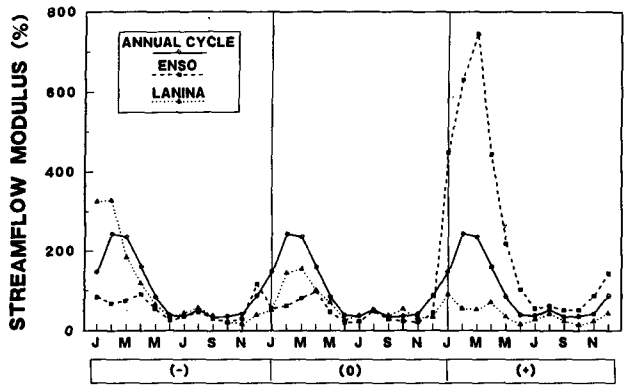

FIG. 7. Regional composites of the T1ENSO (shown by dashed lines) and La Niña events (shown by dotted lines) along with the annual cycle (shown by solid lines), which all are based on the modular coefficients (shown by dotted lines).

formed and plotted along with the regional annual cycle (Fig. 7). Examination of this figure reveals two fundamental features. First, for a typical streamflow behavior during T1ENSO events, a suppressed positive hump of the annual cycle with a relatively low variation during both year (−) and year (0) is followed by an enormously enhanced positive hump of the annual cycle with an increase in variation with respect to the annual mean. This enhancement of magnitudes is concurrent with the previously detected wet seasonal signal. Second, for typical streamflow behavior during La Niña events, a somewhat increased amplitude during year (−) precedes a decreased amplitude during year (0) in the annual cycle. During year (+), a low variation and strongly suppressed peaks in the annual cycle are obvious. An opposite tendency in monthly streamflow fluctuations between the T1ENSO and La Niña composites during years (−), (0), and (+) are noticeable. In summary, Fig. 7 suggests that the tropical heating anomalies modulate the annual streamflow cycle within the PSW region without causing a major seasonal shift (i.e., more than one or two months).

b. *Hypergeometric model*

The probability of a random occurrence of the wet (dry) season in Fig. 3 (Fig. 4) during T1ENSO (La Niña) events was tested using the hypergeometric distribution. A cumulative probability computed from the hypergeometric distribution gives an occurrence significance level of the relationship previously defined for both extreme phases of the SO. Each value of the ITS (seasonally averaged streamflow lognormal percentiles) is considered as a binomial variable (X), which simply counts the number of successes in a sequence of independent, identical trials or observations resulting in either success or failure at each time. Two cases, A and B, are tested. In case A, for the T1ENSO (La Niña) streamflow relationship, a success is defined as an ITS value above (below) the 50th percentile. In case B, our interest is extreme streamflow conditions; thus, for the T1ENSO (La Niña) streamflow relationship, a success is defined as the occurrence of a wettest (driest) season in any year whose positive (negative) departure from the median is greater (lower) than the 67.7 (31.9) percentile in the ITS. A cumulative probability (P) that at least m successes are obtained in n trials from a finite population of size N containing k successes is computed from (2) (Yevjevich 1972). This model was also used by Kiladis and Diaz (1989) and Ropelewski and Halpert (1989) in a similar manner to case A:

$$P(X \geq m) = F_x(m, N, n, k) = \sum_{i=m}^{n} \frac{\binom{k}{i}\binom{N-k}{n-i}}{\binom{N}{n}}. \quad (2)$$

In a particular application of this probability distribution model in this study, the parameters are defined as follows: for case A, n is the number of T1ENSO (La Niña) events, and m is the number of years that an ITS value associated with T1ENSO (La Niña) events is greater (lower) than the median. For case B, n is the number of years that an ITS value falls into the upper (lower) 20% of the distribution of the ITS values, and m is the number of years in which an ITS value associated with T1ENSO (La Niña) events falls into the upper (lower) 20% of the distribution. For both cases, N, the total number of observations in the ITS, is the same, and k, the number of success, has been previously defined. Table 1 summarizes the probability assessments for the relationships. In case A, the application of the hypergeometric distribution model results in a very low level of probability of occurrence by chance (less than 0.02) for both events. In case B, the probability is very low only for T1ENSO events. The extreme wet streamflow conditions appear to be almost exclusively related to T1ENSO events in the 41-yr period. Overall results in Table 1 are also consistent with

TABLE 1. Probabilistic assessments for significance level based on the hypergeometric distribution using the index time series. The explanations for the other parameters and cases are given in the text.

Event	Case	N	k	n	m	P_H
T1ENSO	A	41	15	7	7	0.0003
	B	41	8	8	6	0.0002
La Niña	A	41	27	8	8	0.0232
	B	41	8	8	3	0.1724

the high confirmation rates (100% for both events) for temporal consistency of the signals. All of this implies that the relationship depicted in the aggregate composites is probably due to nonrandom forcing mechanisms (i.e., the tropical thermal anomalies).

c. Cross correlation analysis

If both extreme events of the SO really influence streamflow in the PSW region, then it is appropriate to quantify the degree of this influence by a cross-correlation analysis between the series of streamflow and the SOI. In general, a cross-correlation analysis is used to determine the time-dependence structure or the strength of the linear relationship between the two time series. Either extreme of the SO has been known to be a precursor to certain hydroclimatologic fluctuations in the western United States. Koch et al. (1991) attempted to quantify these fluctuations by correlating seasonal streamflow with different seasonal SOI values that were averaged over two-, three-, four-, five-, and six-month periods. Since the signal-to-noise ratio of the SOI improves from 1.44 for monthly data to 1.97 for seasonal data (Trenberth 1984), it is reasonable to average the SOI values over a season having a minimum three-month period in the correlation analysis.

In assessing a confidence level for a computed cross-correlation coefficient (CCC), the null hypothesis regarding the population CCC, (H_0: $\rho_1 = 0$), is tested using a symmetric distribution of CCC. Assuming that both variables are characterized by the normal distribution and are selected randomly from their respective populations, the following statistic, t, complying with Student's distribution can be used:

$$t = \frac{r_1(N_e - 2)^{1/2}}{(1 - r_1^2)^{1/2}}, \qquad (3)$$

in which N_e is the reduced or effective sample size that accounts for the effect of serial correlation existing in each of the two series. This is attributed to the fact that a serially correlated sample of size N possesses less information about a process than a purely random sample of the same size. The term N_e in (3) can be approximated by

$$N_e = \frac{N - k}{1 + 2R_1R'_1 + 2R_2R'_2 + \cdots + 2R_kR'_k}, \qquad (4)$$

where R_k and R'_k are the respective lag-k serial correlation coefficients for the two time series. Only R_k and R'_k, which are statistically significant at the 95% level according to Anderson's test, are included in the denominator of (3), and the remaining terms are considered to be zero. Since r_k can be significantly greater or smaller than zero, a two-tailed test at the 0.05 level has been carried out. Thus, the null hypothesis is rejected if t is larger than $t_{0.975}$ with $(N_e - 2)$ degrees of freedom.

We attempted to capture a period for averaging the SOI along the entire preceding year of the seasonal T1ENSO signal at which the association between streamflow, SOI, and the time lag are substantially large. Our motivation to focus on the seasonal SOI (a period of 3 to 12 months) and the seasonal time lag (a time interval of 0 to 9 months) is based on three factors: (i) an ENSO is a slowly progressing event, (ii) a low-frequency mode of atmosphere might play an important role as a long range predictor (Cayan and Peterson 1989), and (iii) the timing of the T1ENSO signal provides insight that the associated tropical influences were in effect in earlier seasons. The Pearson's product-moment formula (Yevjevich 1972) was used to compute a lag-k CCC, denoted by r_1, between the ITS and the seasonal SOI series. The operational version of the SOI was used and provided in a standardized form by the Climate Analysis Center (Ropelewski and Jones 1987).

Ten cases with a total of 55 scenarios were analyzed by forming different SOI periods. In the first scenario of case 1, the SOI was averaged over a three-month period spanning December to February and correlated with the ITS (the lognormal streamflow percentiles averaged over the December–July season) to obtain a lag-1 CCC. For each CCC, there is one corresponding significance level computed from (3). In the second scenario of case 1, the averaging period was increased by one month from the end to obtain a four-month period (December to March). This new SOI period is used to compute another lag-1 CCC, and so on. The averaging process continues until the ending month reaches November and the final period in case 1 possesses a period of 12 months. Thus, there are a total of ten scenarios in case 1.

In case 2, the beginning of the SOI averaging period was moved forward by one month; now there are nine scenarios to consider. For example, the January–March period is the first scenario in case 2, and so on. By performing similar modifications to the remaining cases, a total of 55 CCCs are calculated. The results of this analysis are presented in Table 2 as the CCC values. The significance levels have not been shown for brevity. A CCC value of −0.26 or lower, however, has been determined as the threshold for the 90% significance level based on Student's t-test. Two criteria were established in choosing a favorable SOI season(s): first, the minimum length of season and second, the last month of that season's being as far as possible from the beginning of the T1ENSO season. Although this analysis was performed on the ITS (a regional series), the outcomes also enable us to determine a proper SOI season, which can be used as either a predictor variable (for forecasting purposes) or as an independent variable (for a cause–effect analysis). Thus, a relationship is established between the SOI and the December–July

TABLE 2. Cross-correlation coefficients (CCC) between the lognormal streamflow percentiles averaged over the December–July season and the SOI averaged for different lengths of seasons in the preceding year in the PSW region. The value in the box indicates a simultaneous CCC for the December–April season with a significance level in parenthesis.

LS	C1 Dec	C2 Jan	C3 Feb	C4 Mar	C5 Apr	C6 May	C7 Jun	C8 Jul	C9 Aug	C10 Sep
3	−0.08	−0.22	−0.34	−0.42	−0.34	−0.28	−0.34	−0.37	−0.45	−0.50
4	−0.20	−0.28	−0.35	−0.41	−0.34	−0.33	−0.35	−0.43	−0.49	
5	−0.26	−0.30	−0.37	−0.41	−0.37	−0.34	−0.40	−0.47		
6	−0.27	−0.33	−0.38	−0.42	−0.37	−0.39	−0.44			
7	−0.30	−0.34	−0.40	−0.42	−0.41	−0.42				
8	−0.32	−0.37	−0.40	−0.45	−0.44					
9	−0.35	−0.38	−0.43	−0.48						
10	−0.37	−0.42	−0.46							
11	−0.40	−0.45								
12	−0.44						Lag-0: −0.335 (96.8%)			

LS: Length of season (over which the SOI is averaged, in months)
C1, C2,..: Case number with the beginning month for the SOI averaging season

seasonal streamflows at an individual station within the PSW.

Except for the first two scenarios in case 1 and the first in case 2, all other CCCs were found to be highly significant in the PSW region (Table 2). A three-month period of March–May in the previous year of the seasonal T1ENSO signal was suggested here as a desirable period to analyze the December–July averaged streamflow series in the PSW. The associated time lag and the portion of explained variance are six months and 18%, respectively. A careful examination of Table 2 indicates that the inclusion of October in the SOI averaging period increases the relevant CCCs from 0.03 to 0.08. A similar but weak tendency has also been observed for August (three months earlier than the onset of the T1ENSO signal period) with an 0.01 to 0.06 increase in the CCC magnitude. The lag-0 CCC, equal to −0.335, was found to be significant at the 3% level.

Similarly, Cayan and Webb (1992) found significant negative correlation between the SOI and a large region of snowpack and streamflow in the southwest United States (Arizona, New Mexico, southern Utah, Nevada, and California). This negative correlation (summer SOI leads December–August streamflow) appeared in two halves of the sample—before and after 1955. On the monthly timescale, Webb and Betancourt (1990) found significant simultaneous and four- to six-month lag relationships between precipitation in Tucson, Arizona, and the Line Islands. They attributed significant correlations for the same month to the direct association with tropical cloud masses heading in a northeast direction from the central equatorial Pacific Ocean. This means that the tropical convection in this area enhances the subtropical jet stream into the southwest United States, producing more intense storm systems. While some tropical moisture may be advected into North America by these systems, the dynamical effect of increased jet activity is more important in the teleconnection mechanisms.

d. Mann–Whitney U test

It is of interest to determine whether there is a significant difference in the magnitude of seasonal streamflow (averaged over the December–July season) between the years associated with T1ENSO and La Niña events. For this analysis, original monthly streamflows are used to calculate the average of the December–July season for each year at an individual station. Of these 41 values, seven corresponding to T1ENSO signal years (i.e., 1952, 1958, and so on) and eight corresponding to La Niña signal years (i.e., 1951, 1956, and so on) are collected in subset I and subset II, respectively. Since during the warm and cold event signal years the distribution of mean seasonal values is not known a priori and the size of each sample is small, we used a nonparametric statistical technique. A rank-sum test known as the Mann–Whitney U, alternative to the classical t test, is used to infer whether the two independently drawn samples come from the same population (Davis 1973). The null hypothesis can be set as the equality of the subset I and subset II means versus the alternative hypothesis of inequality of the means. The data in the two samples are combined and ranked from the smallest to the highest. Whenever there is a tie among the ranks, the average of them is assigned for each of the tied values. This test is based on the statistic U given as

$$U = mn + \frac{m(m+1)}{2} - R_1, \tag{5}$$

where m and n are the respective size of subset I and subset II, and R_1 is the sum of the ranks assigned to the members of subset I. If the null hypothesis is correct,

it can be shown that the distribution of U has a mean, μ_U, and a standard deviation, σ_U, which can be determined as follows:

$$\mu = \frac{mn}{2}; \quad \sigma_U = \left(\frac{mn(m+n+1)}{12}\right)^{1/2}. \quad (6)$$

Moreover, if both m and n are greater than 8, the distribution of U is approximately normal. Then the test statistic can be changed to a z score using $z_\alpha = (U - \mu_U)/\sigma$, where α is the level of significance.

In the particular application of this test, μ_U and σ_U are equal to 28 and 8.6, respectively, while the z score is, on the average, equal to -2.8. The difference in the means is significant at the 99% or higher level for 34 of 50 streamflow records. Only five out of 50 stations had an insignificant z score (lower than the 90% level). The same test for the seasonal La Niña signal yielded results slightly better than those for the T1ENSO signal. Except for one station, all other stations had a z score significant at the 92% or higher level. Last, the same test was also applied to the original annual streamflow values. This resulted in significance levels as high as the two earlier analyses for every station with the exception of two that had an 85% significance level. These results suggest that the mean of the average warm signal season associated with T1ENSO events is undoubtedly different (in fact larger) than those associated with La Niña events. This is also true for the annual averages.

5. Conclusions

Composite streamflow anomalies during T1ENSO and La Niña events of the SO have been analyzed for 50 streamflow stations across the Pacific Southwestern United States. The influences of T1ENSO and La Niña events taking place in the central and eastern Pacific Ocean on streamflow in the PSW have been documented with respect to the geographical extent, sign, and magnitude of seasonal anomalies. The hypothesized tropical influences have also been characterized as an enhancement (suppression) of the annual cycle during the subsequent year that follows the T1ENSO (La Niña) phenomena. Statistical evidence confirms the results of seasonal signal for both phases of the SO with a high statistical significance level. Extreme wet streamflow conditions for the December–July season are significantly related to the T1ENSO events. This indication is also consistent with the major dry and wet spells in Arizona that were categorized by Diaz (1983) using the Palmer Index. The seasonal SOI, lasting between 3 and 12 months in the previous year of the T1ENSO signal, has been found to be significantly correlated with the current seasonal December–July streamflow. This suggests that the seasonal SOI could be a useful predictor for streamflow. Furthermore, significantly different means of seasonal streamflow averages for the warm and cold episodes demonstrate a sign opposition. This is consistent with the expected biennial fluctuation during the SO extreme cycle.

The determination of a typical streamflow fluctuation during the lifetime of either extreme of the SO also provides a practical way of predicting streamflow one or two seasons in advance. For example, the most recent El Niño episode (1991–92) can be categorized as a Type 1 event (H. Diaz 1992, personal communication). Highly wet conditions during the first half of 1992 in the Southwest and California regions (NWS 1992) were anticipated by the authors during the summer and fall of 1991.

Acknowledgments. The authors wish to thank personally Dr. George Kiladis, University of Colorado/CIRES, and Dr. Henry Diaz, NOAA/ERL, for their helpful discussions. We appreciate Dr. Daniel Cayan, Scripps Institute of Oceanography, who reviewed and improved the quality of the manuscript. The suggestions and questions of two anonymous reviewers are gratefully acknowledged. Special thanks are due to Professor Roy W. Koch for providing the SOI time series. Mrs. Hasibe Kahya and Mr. Fabrice Cuq are gratefully acknowledged for data preparation and plotting maps. Funding for this project was provided by the Metropolitan Water District of Southern California under Agreement 2501.

REFERENCES

Aceituno, P., 1992: El Niño, the Southern Oscillation, and ENSO: Confusing names for a complex ocean–atmosphere interaction. *Bull. Amer. Meteor. Soc.*, **73**, 483–485.

Andrade, E. R., and W. D. Sellers, 1988: El Niño and its effect on precipitation in Arizona. *J. Climatol.*, **8**, 403–410.

Angell, J. K., and J. Korshover, 1987: Variability in United States cloudiness and its relation to El Niño. *J. Climate Appl. Meteor.*, **26**, 580–584.

Cayan, D. R., and D. H. Peterson, 1989: The influence of north Pacific atmospheric circulation on streamflow in the West, PACLIM. *AGU Monogr.*, No. 55, 375–397.

——, and R. H. Webb, 1992: El Niño/Southern Oscillation and streamflow in the western United States. *El Niño: Historical and Paleoclimatic Aspects of the Southern Oscillation*, H. F. Diaz and V. Markgraf, Eds., Cambridge University Press, 29–88.

Conrad, V., and L. W. Pollak, 1950: *Methods in Climatology*. Harvard University Press, 459 pp.

Davis, J. C., 1973: *Statistics and Data Analysis in Geology*. John Wiley and Sons, 646 pp.

Diaz, H. F., 1983: Drought in the United States: Some aspects of major dry and wet periods in the contiguous United States, 1895–1981. *J. Climate Appl. Meteor.*, **22**, 3–16.

Douglas, A. E., and P. J. Englehart, 1981: On a statistical relationship between autumn rainfall in the central equatorial Pacific and subsequent winter precipitation in Florida. *Mon. Wea. Rev.*, **109**, 2377–2382.

——, and ——, 1984: Factors leading to the heavy precipitation regimes of 1982–1983 in the United States. *Proc. of the Eighth Annual Climate Diagnostics Workshop*, Washington, DC, 42–54.

Ely, L. L., Y. Enzel, and D. R. Cayan, 1992: Anomalous atmospheric circulation and large winter floods in six subregions of the

southwestern United States. *Proc. of the Eighth Annual Pacific Climate (PACLIM) Workshop,* 179–186.

Fu, C., H. F. Diaz, and J. O. Fletcher, 1986: Characteristics of the responses of SST in the central Pacific associated with warm episodes of the Southern Oscillation. *Mon. Wea. Rev.*, **114,** 1716–1738.

Hales, J. E., Jr., 1974: Southwestern United States summer monsoon source, Gulf of Mexico or Pacific Ocean? *Weatherwise,* **24,** 148–155.

Hsu, C. F., and J. M. Wallace, 1976: The global distribution of the annual and semiannual cycles in precipitation. *Mon. Wea. Rev.*, **104,** 1093–1101.

Kahya, E., and J. A. Dracup, 1993a: U.S. streamflow patterns in relation to the El Niño/Southern Oscillation. *Water Resour. Res.*, **29,** 2491–2503.

——, and ——, 1993b: The relationships between ENSO events and California streamflows. *Proc. of The World at Risk: Natural Hazards and Climate Change,* American Institute of Physics, 86–95.

Kiladis, G., and H. Diaz, 1989: Global climatic anomalies with extremes in the Southern Oscillation. *J. Climate,* **2,** 1069–1089.

Koch, R. W., C. F. Buzzard, and D. M. Johnson, 1991: Variation of snow water equivalent and streamflow in relation to the El Niño/Southern Oscillation. *Proc. Western Snow Conf.,* Juneau, 37–48.

NWS, 1992: *Water Supply Outlook for the Western United States.* National Oceanic and Atmospheric Administration, Office of Hydrology.

Philander, S. G., 1990: *El Niño, La Niña, and the Southern Oscillation.* Academic Press, 293 pp.

Quinn, W. H., D. O. Zopf, K. S. Short, and R. T. W. Kuo Yang, 1978: Historical trends and statistics of the Southern Oscillation, El Niño, and Indonesian drought. *Fish. Bull.*, **76,** 663–678.

Rasmusson, E. M., and T. H. Carpenter, 1982: Variations in tropical sea surface temperature and surface wind fields associated with the Southern Oscillation/El Niño. *Mon. Wea. Rev.*, **110,** 354–384.

Rayner, J. N., 1971: *An Introduction to Spectral Analysis.* Pion Limited, 174 pp.

Ropelewski, C. F., and M. S. Halpert, 1986: North American precipitation and temperature patterns associated with the El Niño/Southern Oscillation (ENSO). *Mon. Wea. Rev.*, **114,** 2352–2362.

——, and ——, 1987: Global and regional scale precipitation patterns associated with the El Niño/Southern Oscillation. *Mon. Wea. Rev.*, **115,** 1606–1626.

——, and C. F. Jones, 1987: An extension of the Tahiti–Darwin Southern Oscillation index. *Mon. Wea. Rev.*, **115,** 2161–2165.

——, and M. S. Halpert, 1989: Precipitation patterns associated with the high index phase of the Southern Oscillation. *J. Climate,* **2,** 268–284.

Schonher, T., and S. E. Nicholson, 1989: The relationship between California rainfall and ENSO events. *J. Climate,* **2,** 1258–1269.

Scott, C. M., and M. D. Shulman, 1979: An areal temporal analysis of precipitation in the northeastern United States. *J. Appl. Meteor.*, **18,** 627–633.

Trenberth, K. E., 1984: Signal versus noise in the Southern Oscillation. *Mon. Wea. Rev.*, **112,** 326–332.

van Loon, H., and R. Madden, 1981: The Southern Oscillation. Part I: Global associations with pressure and temperature in Northern winter. *Mon. Wea. Rev.*, **109,** 1150–1162.

Wallis, J. R., D. P. Lettenmaier, and E. F. Wood, 1991: A daily hydroclimatological dataset for the continental United States. *Water Resour. Res.*, **27,** 1657–1663.

Webb, R. H., and J. L. Betancourt, 1990: Climatic variability and flood frequency of the Santa Cruz River, Pima County, Arizona. U.S. Geological Survey Open-File Report 90-553, 69 pp. [Available from Federal Center, Box 25425, Denver, CO 80225.]

Yevjevich, V., 1972: Probability and Statistics in Hydrology. Water Resources Publication, Fort Collins, CO, 302 pp. [Available from P.O. Box 2841, Littleton, CO 80161.]